Temperature Insensitive Refractometer Using Core and Cladding Modes in Open-Top Ridge Waveguide

Xiaoli Dai, Robert B. Walker, Stephen J. Mihailov, Chengkun Chen, Chantal Blanchetière, Claire L. Callender, and Jacques Albert

***Abstract*—In order to overcome the well-known limitation of temperature instability in Bragg grating waveguide sensors, a temperature insensitive open-top ridge waveguide refractometer is developed by using a cladding mode resonance as a temperature reference. The relative shift of the core mode resonance to cladding mode resonance is used to measure the refractive index of substances under test. Specifically, the device fabricated here produces a relative resonance shift of 1 pm for every 5×10^{-4} of measured index change, with a temperature sensitivity ~ 0.5 pm/°C.**

***Index Terms*—Bragg grating, cladding mode, core mode, refractive index sensor, ridge waveguide, temperature insensitive.**

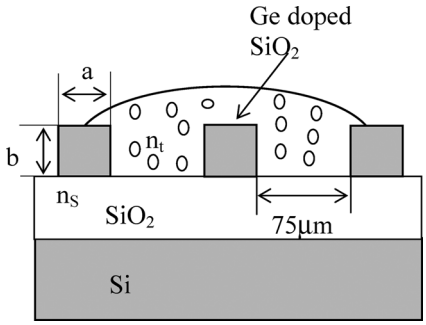

Fig. 1. The structure of open-top ridge waveguide without top cladding.

I. Introduction

WITH THEIR miniature size, noninvasive and rapid detection, Bragg grating refractometric sensors are becoming useful tools for chemical analysis and biomedical testing. Measurements from Bragg grating-based refractometers, however, often can be distorted by fluctuations in the ambient temperature. For temperature insensitive sensors based on fiber Bragg gratings, several techniques have been proposed to discriminate between Bragg resonance spectral shifts associated with refractive index measurements and those induced by fluctuations in temperature. These techniques are implemented by using: a second Bragg grating in a side-polished fiber Bragg grating refractometer [1], [2], higher order modes in an etched-core of a fiber Bragg grating sensor [3], [4], and higher order modes in a tilted fiber Bragg grating sensor [5]–[9]. In our previous work [10], a highly sensitive waveguide Bragg grating (WBG) sensor for measuring small changes in the refractive index of a surrounding liquid was developed. By using an open-top ridge waveguide with a small core, the evanescent field interaction of the guided mode with the liquid analyte was enhanced. The sensitivity measured via a shift in the resonance wavelength of the Bragg grating was as high as 1 pm of wavelength shift for a change of 4×10^{-5} in the liquid refractive index on the top layer. However, the device was sensitive to temperature change as the Bragg wavelength shifted with temperature (~ 11 pm/°C in silica waveguides). In this work, we propose a technique for creating a temperature insensitive refractometer that utilizes core and cladding modes in an open-top ridge waveguide architecture in order to discriminate between changes in temperature and refractive index.

The structure of the open-top ridge waveguide is as shown in Fig. 1. In Fig. 1, the center ridge waveguide with the Bragg grating is tested as a refractometer by coupling the light source into the end of the waveguide. The function of the two adjacent waveguides is to act as a barrier and to partially prevent the liquid from flowing away from the waveguide with the grating. The adjacent waveguides do not contribute to the device performance. The guided light of the center waveguide couples evanescently into the surrounding liquid through the top and sides of the waveguide. The three waveguides shown in Fig. 1 have the same dimension and are separated by 75 μm. Three different sets of waveguide dimensions were used in the experiments: $7.7\,\mu\text{m} \times 5.6\,\mu\text{m}$, $6.6\,\mu\text{m} \times 5.6\,\mu\text{m}$, and $5.7\,\mu\text{m} \times 5.6\,\mu\text{m}$. As an open-top ridge waveguide exposes three sides of the core ($\sim 270°$) to a surrounding liquid, the core modes associated with these structures exhibit higher sensitivity to the index of the analyte liquid than is present in side-etched waveguide designs. When a Bragg grating is induced in the core of an open-top ridge waveguide, core and cladding resonances are observed when the light modes guided by the core and undercladding are phase matched by the grating structure. Both the core and cladding resonances are sensitive to the liquid refractive index on the top layer of the open-top ridge waveguide. However, because modes of the undercladding have a different degree of exposure and are somewhat shielded by the waveguide itself, the sensitivity of the cladding modes to the refractive index of the analyte liquid is different from the sensitivity of the core mode. The core and cladding mode sensitivities to temperature fluctuations, however, are more closely matched as the thermo-optic

Manuscript received November 30, 2006; revised February 22, 2007; accepted February 27, 2007. The associate editor coordinating the review of this paper and approving it for publication was Dr. Richard Fair.

X. Dai, R. B. Walker, S. J. Mihailov, C. Blanchetière, and C. L. Callender are with the Communications Research Centre, Ottawa, ON K2H 8S2, Canada (e-mail: xiaoli.dai@crc.ca; robert.walker@crc.ca; claire.callender@crc.ca).

C. Chen and J. Albert are with the Department of Electronics, Carleton University, Ottawa, ON K1S 5B6, Canada (e-mail: chchen@doe.carleton.ca; jacques_albert@carleton.ca).

Color versions of one or more of the figures in this paper are available online at http://ieeexplore.ieee.org.

Digital Object Identifier 10.1109/JSEN.2008.918172

coefficients of the silica waveguide core and cladding materials are similar to each other. These characteristics can be used to decouple fluctuations of the Bragg resonance of the core mode due to temperature from those changes that are due to variation in the refractive index of the analyte liquid.

In the experiments presented here, the variation of the cladding and core resonances are investigated as a function of temperature and the external refractive index n_t. In the analysis, simulations of the field distributions of the core and cladding resonances as a function of n_t are performed and are consistent with the measurement results. A theoretical model is developed to investigate the performance of some potential waveguide structures. Relationships between the waveguide core size, refractive index distribution, as well as the relative evanescent sensitivity of the core and cladding modes are examined. As a result, we find that decreasing the waveguide core size, especially when the effective index of the waveguide is close to the expected refractive index of the analyte, can enhance the sensitivity of the refractometer.

II. Experimental Results

As shown in Fig. 1, ridge waveguides were fabricated in a 6 ± 0.5 μm thick Ge-doped SiO_2 layer grown by flame hydrolysis deposition (FHD) on a 7 μm layer of thermal silicon dioxide on silicon. The ridges were produced using standard photolithography and reactive ion etching (RIE) using a CHF_3/O_2 gas mixture. The core layer index n_g was measured before etching by prism coupling at 1537 nm to be 1.4545 ± 0.0004. The bottom cladding index n_s was 1.4436, which was $0.75 \pm 0.07\%$ less than n_g. The dimensions of the waveguides, as measured using scanning electron microscopy were 7.7 μm $\times$ 5.6 μm, 6.6 μm $\times$ 5.6 μm, and 5.7 μm $\times$ 5.6 μm, respectively. The distance between two adjacent ridges was 75 μm. On a wafer patterned with different core size ridge waveguides, Bragg gratings were written using a single zero-order nulled phase mask and an ArF excimer laser with an emission wavelength of 193 nm. With a UV cylindrical lens, the laser beam was focused to a spot size of 5 mm $\times$ 300 μm onto the wafer surface. A strong Bragg grating with index modulation $\Delta n \sim 9 \times 10^{-4}$ was induced in the hydrogen loaded 6.6 μm $\times$ 5.6 μm waveguide with 40 Hz, 100 mJ/cm^2/pulse of polarized UV irradiation (oriented normal to the waveguide axis). The laser beam was polarized to reduce the birefringence of the device [10]. The total UV exposure for the fabrication of the Bragg grating with -21 dB transmission and 0.7 nm bandwidth is 1 kJ/cm^2. The section of the waveguide that contains the Bragg grating with the 5 mm length is covered with the analyte liquid entirely when the refractive index changes of the liquid were measured. The experimental setup is shown in Fig. 2. To monitor the changes of core and cladding modes with the refractive index of the liquid analyte and temperature, the broadband light from a 980 nm-pumped erbium-doped fiber was coupled via a single-mode fiber into the core of the open-top waveguide. The transmitted light was out-coupled to a single-mode fiber and monitored by using an optical spectrum analyzer.

First, the characterization of the device as a refractometer was carried out. Cargille liquids were used to test the devices at 22 °C. Liquids with different refractive indices n_t were dropped onto the top surface of the waveguide. The transmission spectra

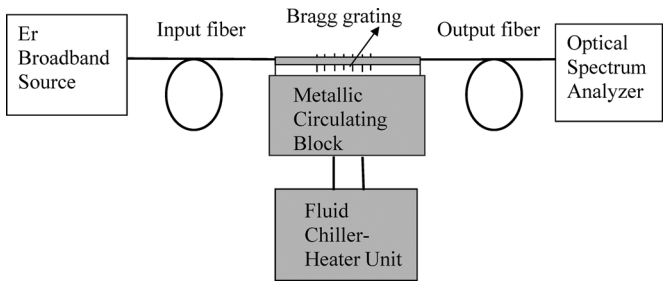

Fig. 2. The configuration of measurement setup.

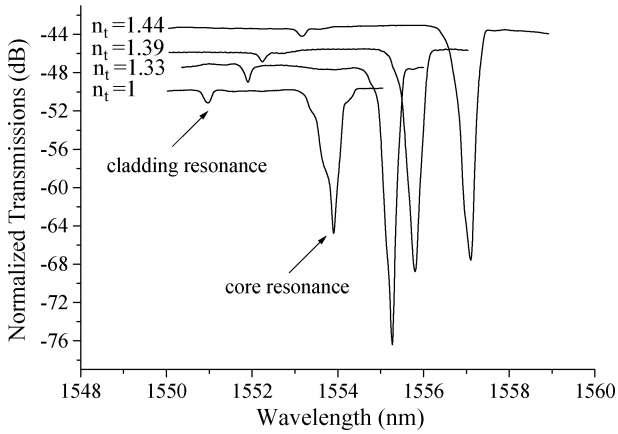

Fig. 3. The spectra of core and cladding Bragg resonance shifts with the change of the refractive index of the analyte liquid.

of the device having waveguide core size of 6.6 μm $\times$ 5.6 μm is shown in Fig. 3. For gratings that were written with their planes orthogonal to the waveguide axis, as presented here, much stronger coupling to the core mode as opposed to the cladding mode was observed. From the point-of-view of utilizing both core and cladding modes resonances to decouple temperature and index change information, it is desirable to increase the strength of the cladding mode resonance making it more easily detectable. This can be easily achieved by blazing or tilting the grating slightly with respect to the optical axis of the waveguide [9]. Both core and cladding mode resonances were sensitive to changes of the analyte index n_t. From 1 to 1.44, the core mode wavelength shifted more than the cladding mode wavelength resulting in a core-cladding mode wavelength difference $\Delta\lambda_{co-cl}$. Unlike similar devices in optical fiber, the Bragg resonance of the core mode was more sensitive than the cladding mode resonance to the refractive index change of the liquid on top of the waveguide. Devices with waveguide core sizes of 7.7 μm $\times$ 5.6 μm, and 5.7 μm $\times$ 5.6 μm were also tested. The results were plotted in Fig. 4. It is shown that the sensitivity to the analyte increased with decreasing waveguide core width. As the sensitivity S_e is defined as $\Delta(\lambda_{\text{core}} - \lambda_{\text{cladding}})/\Delta n_t$, it is dominated by the change of the core mode evanescent sensitivity that increases with decreasing core width [10]. The small core size 5.7 μm $\times$ 5.6 μm device had the highest sensitivity. The sensitivity increased slowly for low analyte indices, but increased more rapidly as n_t approached that of the waveguide core n_g. The sensitivity measured via the variation of $\Delta\lambda_{co-cl}$ with n_t corresponded to a 1 pm increase of $\Delta\lambda_{co-cl}$ for a change of n_t of 5×10^{-4}.

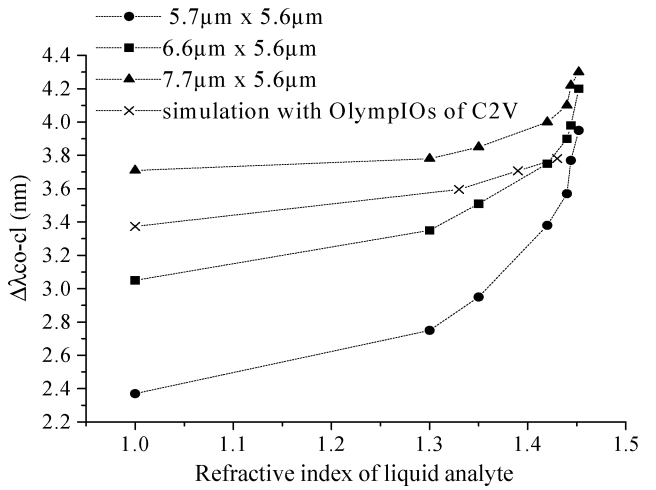

Fig. 4. The difference of cladding and core resonances as a function of the test liquid refractive index for the devices with waveguide cores were $7.7\ \mu\text{m} \times 5.6\ \mu\text{m}$, $6.6\ \mu\text{m} \times 5.6\ \mu\text{m}$, and $5.7\ \mu\text{m} \times 5.6\ \mu\text{m}$ denoted by triangles, squares and circles respectively. Simulated responses for a $6.6\ \mu\text{m} \times 5.6\ \mu\text{m}$ are denoted by crosses.

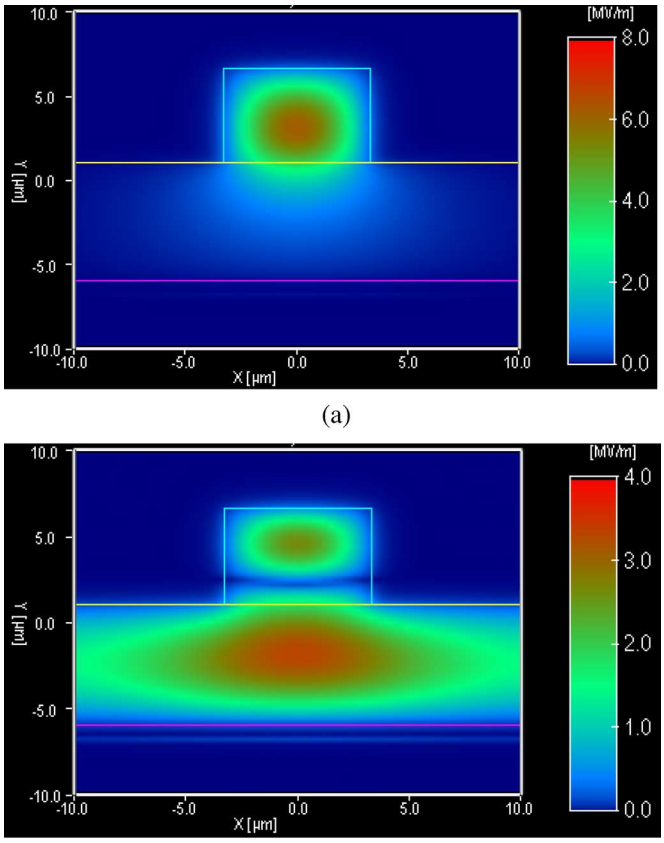

Fig. 5. The simulation results of the field distributions of core mode and cladding mode in TE polarization: (a) core mode and (b) cladding mode.

As a comparison, the field distributions of the core and cladding modes of the waveguide having core dimensions of $6.6\ \mu\text{m} \times 5.6\ \mu\text{m}$, were simulated by a generic finite difference method using the commercial software package *OlympIOs* of $C2V$. The resultant field distributions of the core and cladding modes for the device were shown in Fig. 5. It is clear that the cladding mode is less sensitive to the external index changes

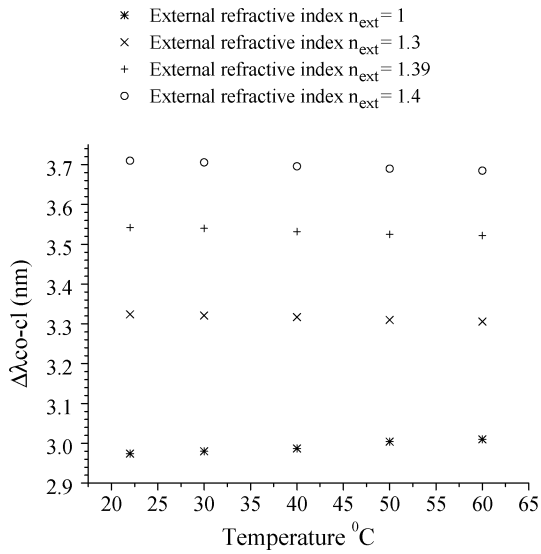

Fig. 6. The test results of the difference of cladding and core mode resonances varying with temperature for the device whose waveguide core is of $6.6\ \mu\text{m} \times 5.6\ \mu\text{m}$.

than core mode, because the cladding mode field is less confined in core layer than in cladding layer. The corresponding $\Delta\lambda_{co-cl}$ as a function of external index resulting from the simulation was also plotted in Fig. 4.

To investigate the temperature stability of the device, the waveguide was mounted on a metallic block in which liquid at a constant temperature could be circulated. The temperature of the device was varied in a stepwise fashion through a fluid chiller-heater unit connected to the metallic circulating block and the temperature was measured at the surface of the block. The variation of $\Delta\lambda_{co-cl}$ with temperature (22 °C–65 °C) was measured for a device with a waveguide core size of $6.6\ \mu\text{m} \times 5.6\ \mu\text{m}$ using index-matching fluids with refractive indexes of 1 (air), 1.3, 1.33, and 1.4, respectively. The results were shown in Fig. 6. The variation of $\Delta\lambda_{co-cl}$ with temperature was $\sim\ 0.5\ \text{pm}/^\circ\text{C}$. The temperature dependence of the cladding mode Bragg resonance was similar to that of the core mode Bragg resonance. With the exception of $n_t\ =\ 1$, the variation of $\Delta\lambda_{co-cl}$ decreased with increasing temperature because of the thermal dependence of the refractive index of the matching oils. For the liquids whose refractive indices are 1.33, 1.39, and 1.40, their index variation with temperature are $-3.6 \times 10^{-4}/^\circ\text{C}$, $-4 \times 10^{-4}/^\circ\text{C}$, and $-4 \times 10^{-4}/^\circ\text{C}$, respectively. For the liquid with the refractive index of 1.40, the refractive index variation with temperature is $-4 \times 10^{-4}/^\circ\text{C}$. By the sensitivity curve of Bragg wavelength difference between core mode and cladding mode versus the analyte n_t in Fig. 4, we have $\text{d}\lambda/\text{dn}_\text{t}\ =\ 2.900$ nm for the refractive index of 1.40. Thus, the change of Bragg wavelength difference between the core mode and cladding mode with the temperature change is about $-1.1\ \text{pm}/^\circ\text{C}$, which is partially compensated by a positive shift resulting from the difference of the thermo-optic and thermomechanical effects in the core and the cladding. The Ge-doped SiO_2 core has higher thermo-optic and thermomechanical effects than the pure SiO_2 cladding. From the experimental results of $n_t\ =\ 1$ in Fig. 6, the positive shift in the Bragg wavelength difference is about $+0.6\ \text{pm}/^\circ\text{C}$. Therefore, the Bragg wavelength difference should change with temperature by about $-0.5\ \text{pm}/^\circ\text{C}$.

III. Discussion

In Bragg grating waveguide structures, the resonant wavelengths of fundamental harmonic backward and forward propagating modes may be written as

$$\lambda_{\mathrm{ResBkwd}} = (n_{\mathrm{eff,In}} + n_{\mathrm{eff,Bkwd}})\Lambda \quad (1)$$

$$\lambda_{\mathrm{ResBkwd}} = (n_{\mathrm{eff,In}} - n_{\mathrm{eff,Fwd}})\Lambda \quad (2)$$

where Λ is the grating period, $n_{\mathrm{eff,In}}$ is the effective refractive index of the incident mode, $n_{\mathrm{eff,Bkwd}}$ is the effective refractive index of the backward propagating coupled mode, $n_{\mathrm{eff,Fwd}}$ is the effective refractive index of the forward propagating coupled mode. The core mode Bragg wavelength is produced when the effective refractive indices of the incident mode and the backward propagating coupled mode are equal to the core effective refractive index of the waveguide. With (1), we have

$$\lambda_{\mathrm{core}} = 2\mathrm{n}_{\mathrm{eff,core}}\Lambda. \quad (3)$$

Cladding mode resonances are produced when the light propagating in the forward direction along the core is coupled into the cladding by the Bragg grating. From (1) for backwards scattering, we have

$$\lambda_{\mathrm{cladding}} = (n_{\mathrm{eff,core}} + n_{\mathrm{eff,cladding}})\Lambda. \quad (4)$$

With this in mind, for scattered core and cladding modes, co-directionally propagating in either the forward or backward direction, the difference in wavelength shift as a function of the analyte index variation Δn_t can be expressed as

$$\Delta(\lambda_{\mathrm{core}} - \lambda_{\mathrm{cladding}})/\Delta n_t = [1-(\Delta n_{\mathrm{eff,cladding}}/\Delta n_{\mathrm{eff,core}})] \times (\Delta n_{\mathrm{eff,core}}/\Delta n_t)\Lambda. \quad (5)$$

We have the relative evanescent sensitivity

$$S = [1 - (\Delta n_{\mathrm{eff,cladding}}/\Delta n_{\mathrm{eff,core}})]\,(\Delta n_{\mathrm{eff,core}}/\Delta n_t). \quad (6)$$

By increasing the values of $[1 - (\Delta n_{\mathrm{eff,cladding}}/\Delta n_{\mathrm{eff,core}})]$, *and* $\Delta n_{\mathrm{eff,core}}/\Delta n_t$, S can be made more sensitive to the change of the analyte n_t. The value of $n_{\mathrm{eff,core}}$ can be obtained by a simple numerical method [12]. The relationship of $n_{\mathrm{eff,cladding}}$ and $n_{\mathrm{eff,core}}$ can be obtained from the experimental results.

Several approaches can be used to analyze ridge waveguide structures [12]–[15] to calculate the effective index $n_{\mathrm{eff,core}}$. In particular, we make use of a simple numerical method [16] previously developed to analyze the dispersion characteristics of guided modes within a strip waveguide. According to this method, the effective index n_{TM} of the guided TM core mode is given by

$$n_{\mathrm{TM}}^2 = \acute{n}_{\mathrm{TM}}^2 - m^2\pi^2/4a^2k^2\left[1 - 2/ak\left(n_g^2 - n_t^2\right)^{1/2}\right] \quad (7)$$

while the effective index n_{TE} of the guided TE core mode is given by

$$n_{\mathrm{TE}}^2 = \acute{n}_{\mathrm{TE}}^2 - m^2\pi^2/4a^2k^2\left[1 - 2/ak\left(n_g^2 - n_t^2\right)^{1/2} + 2\left(n_g^2 - n_t^2\right)^{1/2}/akn_g^2\right] \quad (8)$$

where $k = 2\pi/\lambda$ is a frequency's free-space wave number. $\acute{n}_{\mathrm{TE}}$ and $\acute{n}_{\mathrm{TM}}$ are the effective indices of TE and TM modes associated with the three-layer slab prior to waveguide formation/etching, a is the width of the ridge waveguide, and n_g, n_s, n_t are refractive indices of the core, substrate, and the surrounding regions. Consider how to increase $\Delta n_{\mathrm{eff,core}}/\Delta n_t$ by optimizing the waveguide structure. As outlined in [3], (6) and (7) yield the following expressions for the TM and TE mode:

$$\Delta n_{\mathrm{TM}}/\Delta n_t = \acute{S}_{\mathrm{TM}}(\acute{n}_{\mathrm{TM}}/n_{\mathrm{TM}}) + (n_t/n_{\mathrm{TM}})(m^2\pi^2/4a^3k^3) \times \left[1/\left(n_g^2 - n_t^2\right)^{3/2}\right] \quad (9)$$

$$\Delta n_{\mathrm{TE}}/\Delta n_t = \acute{S}_{\mathrm{TE}}(\acute{n}_{\mathrm{TE}}/n_{\mathrm{TE}}) + (n_t/n_{\mathrm{TE}})(m^2\pi^2/4a^3k^3) \times \left[1/\left(n_g^2 - n_t^2\right)^{3/2} + 1/n_g^2\left(n_g^2 - n_t^2\right)^{1/2}\right] \quad (10)$$

where $\acute{\mathrm{S}}_{\mathrm{TE}} = \partial\acute{\mathrm{n}}_{\mathrm{TE}}/\partial\mathrm{n}_{\mathrm{t}}$ and $\acute{\mathrm{S}}_{\mathrm{TM}} = \partial\acute{\mathrm{n}}_{\mathrm{TM}}/\partial\mathrm{n}_{\mathrm{t}}$. $\acute{\mathrm{S}}_{\mathrm{TE}}$ and $\acute{\mathrm{S}}_{\mathrm{TM}}$ are the sensitivities of TE and TM modes for the three-layer slab prior to waveguide formation/etching. As $\acute{n}_{\mathrm{TE}} \approx n_{\mathrm{TE}}$ and $\acute{n}_{\mathrm{TM}} \approx n_{\mathrm{TM}}$, the first terms in (9) and (10) are dominated by $\acute{S}_{\mathrm{TE}}$ and $\acute{S}_{\mathrm{TM}}$. By the normalized analysis of a slab waveguide evanescent-wave sensor, the expressions of $\acute{S}_{\mathrm{TE}}$ and $\acute{S}_{\mathrm{TM}}$ are given in [10], and optimization results for all slab waveguide sensors are achieved. However, these results cannot be applied directly to ridge waveguides due to the structural difference of the three layer slab waveguides and the ridge waveguides. The structural characteristic of ridge waveguides have a much more significant impact on the second terms of (9) and (10) as is reflected by the presence of parameters a, n_g, and n_t.

Second, let us consider how to obtain the detailed information on the effective index $n_{\mathrm{eff,cladding}}$. With the experimental results, we note that a relationship exists between the ratio of the cladding/core wavelength shifts and the waveguide width a, as illustrated in Fig. 7. This data has been fitted to the quadratic expression provided in (11)

$$\Delta\lambda_{\mathrm{clad}}/\Delta\lambda_{\mathrm{core}} = 0.019193a^2 - 0.169547a + 1.000000 \quad (11)$$

where $5.7\ \mu\mathrm{m} \le a \le 7.7\ \mu\mathrm{m}$. With (3) and (4), we have the expression for $\Delta n_{\mathrm{eff,cladding}}/\Delta n_{\mathrm{eff,core}}$

$$\Delta n_{\mathrm{eff,cladding}}/\Delta n_{\mathrm{eff,core}} = 2\Delta\lambda_{\mathrm{clad}}/\Delta\lambda_{\mathrm{core}} - 1 = 0.038386a^2 - 0.339094a + 1. \quad (12)$$

Substituting (9), (10), and (12) into (6) yields the expression of the relative evanescent sensitivity S

$$\begin{aligned} S_{\mathrm{TM}} &= (0.339094a - 0.038386a^2) \times \left\{\acute{S}_{\mathrm{TM}} + (n_t/n_{\mathrm{TM}})(m^2\pi^2/4a^3k^3) \times \left[1/\left(n_g^2 - n_t^2\right)^{3/2}\right]\right\} \\ &= \acute{S}_{\mathrm{TM}}(0.339094a - 0.038386a^2) + (0.339094a - 0.038386a^2) \times \left[(n_t/n_{\mathrm{TM}})(m^2\pi^2/4a^3k^3)\left[1/\left(n_g^2 - n_t^2\right)^{3/2}\right]\right. \end{aligned} \quad (13)$$

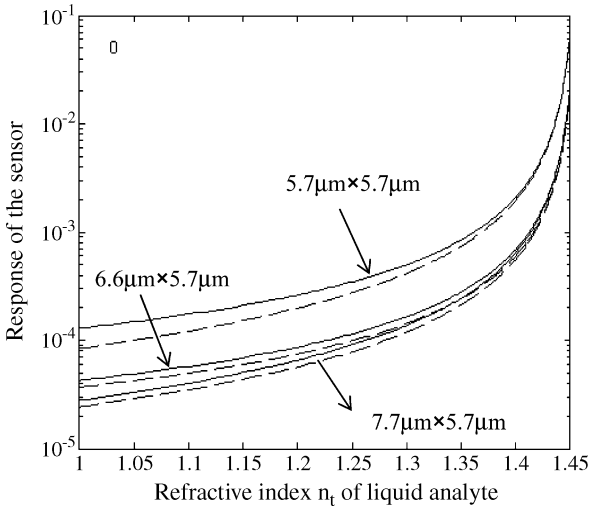

Fig. 7. Analysis results: The response of the sensor changing with waveguide core size and external index in the range of $1 \sim 1.4545$ (solid line for TM mode, dash line for TE mode).

$$
\begin{aligned}
S_{\mathrm{TE}} &= (0.339094a - 0.038386a^2) \\
&\quad \times \left\{ \acute{S}_{\mathrm{TE}} + (n_t/n_{\mathrm{TE}})(m^2p^2/4a^3k^3) \right. \\
&\qquad \left. \times \left[1/\left(n_g^2 - n_t^2\right)^{3/2} + 1/n_g^2\left(n_g^2 - n_t^2\right)^{1/2} \right] \right\} \\
&= \acute{S}_{\mathrm{TE}}(0.339094a - 0.038386a^2) \\
&\quad + (0.339094a - 0.038386a^2) \\
&\quad \times \left[(n_t/n_{\mathrm{TE}})(m^2p^2/4a^3k^3) \right. \\
&\quad \left. \times \left[1/\left(n_g^2 - n_t^2\right)^{3/2} + 1/n_g^2\left(n_g^2 - n_t^2\right)^{1/2} \right] \right. . \qquad (14)
\end{aligned}
$$

$\acute{S}_{\mathrm{TE}}$ and $\acute{S}_{\mathrm{TM}}$ are the sensitivities for the three-layer slab prior to waveguide formation/etching [16]. Their change is related to the thickness variation of the core layer and not to the width variation of the ridge waveguide. To explain how the width variation of the ridge waveguides impacts on the sensitivity, the second terms in (13) and (14) are considered. The results are plotted in Fig. 7 with the analyte index n_t changing from 1 to 1.454 for waveguides with core size are $5.7\ \mu\mathrm{m} \times 5.7\ \mu\mathrm{m}$, $6.6\ \mu\mathrm{m} \times 5.7\ \mu\mathrm{m}$, and $7.7\ \mu\mathrm{m} \times 5.7\ \mu\mathrm{m}$, respectively. Fig. 7 shows that the sensor response increases slowly in the low refractive index region, but increases rapidly as the index of the surrounding medium approaches that of the waveguide. For the range of waveguide widths investigated, the sensitivity also increases as the core width decreases. More specifically, we observe that as the analyte index n_t approaches the core index $n_g = 1.4545$, the relative evanescent sensitivity is maximized. The simulation results in Fig. 7 show the core and cladding mode effective indexes, and their difference shift with the change of the refractive index of the analyte liquid, respectively, they are agreement with the experimental results.

IV. Conclusion

To overcome the temperature instability in a high sensitivity open-top ridge waveguide refractometer that incorporates a Bragg grating, a temperature insensitive refractometer is developed that uses the grating cladding mode resonance as a temperature reference and the relative shift of the grating core mode resonance to measure the refractive index change of a top layer of liquid. As the core and cladding Bragg modes propagate in different locations within the open-top ridge waveguide structure, the core and cladding resonances have similar sensitivities to the temperature but different sensitivities to the external refractive index above the top layer. The shifting of the difference of the core and cladding resonances to the external refractive index change is 1 pm of wavelength shift for 5×10^{-4} change of the external refractive index at a probe wavelength of 1550 nm. The shifting of the difference of the core and cladding resonances to the temperature change is about 0.5 $\mathrm{pm}/^{\circ}\mathrm{C}$. Using the cladding mode resonance as a temperature reference, the relative shift of the core mode resonance is used to measure the refractive index change of the liquid on the top only.

References

[1] K. Schroeder, W. Ecke, R. Mueller, R. Willsch, and A. Andreev, "A fibre Bragg grating refractometer," *Meas. Sci. Technol.*, vol. 12, pp. 757–764, 2001.

[2] D. A. Pereira, O. Frazao, and J. L. Santos, "Fiber Bragg grating sensing system for simultaneous measurement of salinity and temperature," *Opt. Eng.*, vol. 43, no. 2, pp. 299–304, 2004.

[3] X. Shu, B. A. L. Gwandu, Y. Liu, L. Zhang, and I. Bennion, "Sampled fiber Bragg grating for simultaneous refractive-index and temperature measurement," *Opt. Lett.*, vol. 26, pp. 774–776, 2001.

[4] A. N. Chryssis, S. S. Saini, S. M. Lee, H. Yi, W. E. Bentley, and M. Dagenais, "Detecting hybridization of DNA by highly sensitive evanescent field etched core fiber Bragg grating sensors," *IEEE Quan. Elec.*, vol. 11, pp. 864–872, 2005.

[5] S. C. Kang, S. Y. Kim, S. B. Lee, S. W. Kwon, S. S. Choi, and B. Lee, "Temperature-independent strain sensor system using a tilted fiber Bragg grating demodulator," *IEEE Photon. Technol. Lett.*, vol. 10, pp. 1461–1463, 1998.

[6] S. Baek, Y. Jeong, and B. Lee, "Characteristics of short-period blazed fiber Bragg gratings for use as macro-bending sensors," *App. Opt.*, vol. 41, pp. 631–636, 2002.

[7] C. Chen, L. Xiong, A. Jafari, and J. Albert, "Differential sensitivity characteristics of tilted fiber Bragg grating sensors," in *Proc. Optics East 2005*, vol. 6004, p. 60040B-1, Optics East, 2005.

[8] C. F. Chan, C. Chen, A. Jafari, A. Laronche, D. J. Thomson, and J. Albert, "Optical fiber refractometer using narrowband cladding mode resonance shifts," *Appl. Opt.*, vol. 46, pp. 1142–1144, 2007.

[9] G. Laffont and P. Ferdinand, "Tilted short-period fibre-Bragg-grating-induced coupling to cladding modes for accurate refractometry," *Meas. Sci. Technol.*, vol. 12, pp. 765–770, 2001.

[10] X. Dai, S. J. Mihailov, C. L. Callender, C. Blanchetiere, and R. B. Walker, "Ridge-waveguide-based polarization insensitive Bragg grating refractometer," *Meas. Sci. Technol.*, vol. 17, pp. 1752–1756, 2006.

[11] K. S. Chiang, "Dual effective-index method for the analysis of rectangular dielectric waveguides," *Appl. Opt.*, vol. 25, pp. 2169–2174, 1986.

[12] E. A. J. Marcatili, "Dielectric retangular waveguide and directional coupler for integrated optics," *Bell Syst. Tech. J.*, vol. 48, pp. 2071–2102, 1986.

[13] R. Mittra, Y. L. Hou, and V. Jamnejad, "Analysis of open dielectric waveguide using mode-matching technique and variational methods," *IEEE Trans. Microwave Theory Tech.*, vol. MTT-288, pp. 36–43, 1980.

[14] C. Yeh, K. Ha, S. B. Dong, and W. P. Brown, "Single-mode optical waveguides," *Appl. Opt.*, vol. 18, pp. 1490–1504, 1979.

[15] K. S. Chiang, "Dispersion characteristics of strip dielectric waveguides," *IEEE Trans. Microwave Theory Tech.*, vol. 39, pp. 349–352, 1991.

[16] O. Parriaux and G. J. Veldhuis, "Normalized analysis for the sensitivity optimization of integrated optical evanescent-wave sensors," *J. Lightwave Technol.*, vol. 16, pp. 573–582, 1998.

Xiaoli Dai received the B.Eng. and M.Eng. degrees from the Department of Optical Instrument Engineering, Tianjing University of China, Tianjing, China, and the Ph.D. degree from the Department of Electrical and Electronic Engineering, Niigata University, Niigata.

From 1996 to 1999, she was a Research Fellow at the National Research Laboratory of Metrology, Japan. In 2001, she joined in the Communications Research Centre, Ottawa, ON, Canada, as a Research Scientist. Her research interests include fiber Bragg gratings, planar waveguides, and optical measurements.

Robert B. Walker received the B.Eng. degree from Carleton University, Ottawa, ON, Canada, in 1996. He is working towards the Ph.D. degree in physics under the direction of Dr. X. Bao at the University of Ottawa, Ottawa.

After graduation, he was with JDS-Fitel Incorporated, Nepean, ON, Canada, where he helped design fiber-optic packaging and tooling as part of the Components Engineering Group. From 1997 to 2000, he was with Fleet Technology Limited, Kanata, ON, as a member of their Structural Reliability and Risk Group. In 2000, he joined the Optical Communications and Electrophotonics Group of the Communications Research Centre, Canada, as a Research Engineer. He is currently working on a number of projects related to fiber Bragg gratings.

Mr. Walker has been a licensed Professional Engineer in Ontario since 1998.

Stephen J. Mihailov received the B.Sc. degree in physics from Carleton University, Ottawa, ON, Canada, in 1986 and the Ph.D. degree in physics from York University, Toronto, ON, Canada, in 1992.

He was a Natural Sciences and Engineering Research Council of Canada Postdoctoral Fellow from 1992 to 1994, where he conducted research on laser-material processing of polymers and glasses at the L'Université de Bordeaux I, Bordeaux, France, and at Exitech Ltd., Oxford, U.K. From 1994 to 1996, he was with JDS-Fitel Incorporated, Nepean, ON, Canada, where he worked on the development of passive optical component technology and was the project leader for the development of fiber Bragg grating technology. In 1996, he joined the Optical Communications and Electrophotonics Group of the Communications Research Centre, Ottawa, ON, Canada, as a Research Scientist, where he conducted research on network applications of fiber Bragg gratings. He is presently the Research Program Manager of the Optical Communications and Electrophotonics Group at the Communications Research Centre.

Chengkun Chen is currently working towards the Ph.D. degree at the Department of Electronics, Carleton University, Ottawa, ON, Canada. He is working in the group of Prof. J. Albert.

Chantal Blanchetière graduated from Universite de Rennes I, France, in 1994, where she worked on optical materials for far-infrared applications. She worked as a Postdoctorate at Alfred University, Alfred, NY, then as a Research Associate at the National Research Council of Canada. She is currently working as a Research Scientist at Communications Research Centre, Ottawa. Her current interests include optical materials, planar optical devices for photonic applications.

Claire L. Callender received the B.Sc. degree in chemistry from Aberdeen University, Aberdeen, U.K., in 1982 and the Ph.D. degree in physical chemistry from Heriot-Watt University, Edinburgh, U.K., in 1986.

She is currently Project Leader of the Photonic Component Technologies group at the Communications Research Centre, Ottawa, ON, Canada. Her current research is focussed on the development of photonic devices for advanced communications systems and sensors, including silica- and polymer-based planar waveguides, the on-chip integration of microfluidic and lightguiding circuitry, and the use of hybrid material structures for novel photonic device functionality.

Jacques Albert is a Professor at the Department of Electronics, Carleton University, Ottawa, ON, Canada, and Canada Research Chair in Advanced Photonic Components.